PHYSICAL REVIEW B VOLUME 21, NUMBER 5 1 MARCH 1980

Parastriction: A new probe for quadrupolar interactions in rare-earth compounds

P. Morin, D. Schmitt, and E. du Tremolet de Lacheisserie

Laboratoire Louis Neel, Centre National de la Recherche Scientifique, 166X, 38042 Grenoble Cedex, France*

(Received 15 October 1979)

We present a new method called parastriction for investigating the quadrupolar interactions in cubic rare-earth intermetallic compounds. Parastriction measures the rare-earth quadrupolar moment induced by an applied magnetic field through the anisotropic deformation of the lattice. The magnetoelastic coefficients associated with the two principal strain modes (tetragonal and rhombohedral) are thereby obtained. The quadrupolar exchange parameters may be evaluated without any ambiguity for compounds with low magnetic-ordering temperature. Application to the heavy rare-earth—zinc compounds is then given.

I. INTRODUCTION

Magnetoelastic effects and in a more general way quadrupolar pair interactions have been extensively studied over the last few years in cubic rare-earth intermetallic compounds. Due to the strong mixing of the $4f$ wave functions by the crystalline electric field (CEF), an anisotropic reduction of the multipolar moments appears in addition to the anisotropy of the energy: Classical treatments such as those proposed by Trammel[1] for the magnetization process and by Callen and Callen[2] for magnetoelasticity fail, and a quantum treatment must then be developed.

In addition, the Hamiltonian must include the quadrupolar exchange interactions, which have been found to be important in cubic rare-earth intermetallics[3]: for instance, in TmZn (Ref. 4) and TmCd (Ref. 5) they are strong enough to induce a pure quadrupolar ordering which reduces the symmetry. This change of structure is analogous to the magnetostrictive process, in which the spontaneous strain is driven by the magnetic dipolar exchange interactions.

Starting from the full Hamiltonian, it is then possible (i) to diagonalize the Hamiltonian in the ordered range to obtain the average value of the various multipolar moments, and (ii) to perform perturbation calculations in the disordered range. This leads, for instance, to the expression of the magnetic susceptibility or the elastic constants.

To obtain additional information in the disordered range, we derive expressions for the tetragonal and rhombohedral strains induced by an applied magnetic field (Sec. II). This parastriction method was outlined recently.[6] It should be emphasized that the two strain modes can be systematically studied, whilst only the spontaneous strain may be achieved in the ordered range due to the strong anisotropic effects. In addition, for each symmetry, since the strains are as sensitive to the quadrupolar exchange interactions as to magnetoelastic coupling, the separation of the two corresponding coefficients is then possible.

In Sec. III, we present an extensive study of the parastriction in the rare-earth—zinc compounds. Indeed, in these cubic CsCl-type structure compounds the quadrupolar (magnetoelastic and exchange) effects were found to be very large[7]: spontaneous strains up to 1% are driven by magnetostrictive processes for compounds from TbZn to ErZn and result from the quadrupolar ordering[4] in TmZn. Our results allow the determination of both magnetoelastic coefficients for each compound and quadrupolar exchange parameters in some favorable cases.

Variation of the tetragonal and rhombohedral magnetoelastic coefficients will be discussed in Sec. IV. They appear not to follow point-charge estimates in a parallel way to the fourth- and sixth-order CEF terms. As the latter ones they are strongly influenced by the electronic structure, that will be discussed in a following paper, where a tentative estimation of the magnetoelastic coefficients will be performed from the modification of the electronic structure by the strain.

II. THEORY

A. The Hamiltonian

The interpretation of the magnetic properties of the $4f$ shell in a cubic surrounding is based upon the following Hamiltonian $\mathcal{H}$, using the operator-equivalent theorem[8] and the molecular-field approximation:

$$\mathcal{H} = \mathcal{H}_{\mathrm{CEF}} + \mathcal{H}_J + \mathcal{H}_Q + \mathcal{H}_{\mathrm{ME}} + (E_{\mathrm{el}} + E_J + E_Q) \ , \tag{1}$$

$$\mathcal{H}_{\mathrm{CEF}} = A_4^0 \langle r^4 \rangle \beta_J O_4 + A_6^0 \langle r^6 \rangle \gamma_J O_6 = \frac{Wx}{F_4} O_4 + \frac{W(1-|x|)}{F_6} O_6 \ , \tag{2}$$

is the usual cubic CEF Hamiltonian expressed in the fourfold-axes system.[9]

$$\mathcal{H}_J = -g_J \mu_{\mathrm{B}} (\vec{\mathrm{H}} + n g_J \mu_{\mathrm{B}} \langle \vec{\mathrm{J}} \rangle) \vec{\mathrm{J}} \tag{3}$$

includes the Zeeman coupling and the Heisenberg exchange interaction, where n is the molecular-field parameter.

$$\mathcal{H} = -K_1(\langle O_2^0\rangle O_2^0 + 3\langle O_2^2\rangle O_2^2) - K_2(\langle P_{xy}\rangle P_{xy} + \text{cycl.}) \qquad (4)$$

is the quadrupolar exchange Hamiltonian, and

$$\mathcal{H}_{\text{ME}} = -B_1(\epsilon_3 O_2^0 + \sqrt{3}\epsilon_2 O_2^2) - B_2(\epsilon_{xy} P_{xy} + \text{cycl.}) \qquad (5)$$

the one-ion magnetoelastic coupling linear in strain, where we neglect the strain modification of the fourth- and sixth-order CEF terms as well as any two-ions magnetoelastic coupling.[10] Within the harmonic hypothesis, the elastic energy E_{el} is written

$$E_{\text{el}} = \tfrac{1}{2}(C_{11}^0 - C_{12}^0)(\epsilon_3^2 + \epsilon_2^2) + 2C_{44}^0(\epsilon_{xy}^2 + \text{cycl.}) \qquad (6)$$

the C_{k1}^0's being the background elastic constants without magnetic interactions.

$$E_J = \tfrac{1}{2} n (g_J \mu_{\text{B}} \langle \vec{\text{J}} \rangle)^2 \qquad (7)$$

and

$$E_Q = \tfrac{1}{2}K_1(\langle O_2^0\rangle^2 + 3\langle O_2^2\rangle^2) + \tfrac{1}{2}K_2(\langle P_{xy}\rangle^2 + \text{cycl.}) \qquad (8)$$

are corrective energy terms for, respectively, the dipolar and quadrupolar exchange interactions originating in the molecular-field approximation: indeed when summing over the whole crystal exchange arising from Eqs. (3) and (4), the energy relative to a pair of rare-earth ions is counted twice.

B. Perturbation theory

In order to determine in the paramagnetic range, the field dependence of the average values of the second-order Stevens operators O_2^0, O_2^2, and P_{k1}, we have to apply a perturbation theory for successively the two cubic strain modes.

1. *Tetragonal symmetry*

The magnetic field H is applied along a fourfold axis, e.g., z, in the paramagnetic range. So $M = g_J\mu_{\text{B}}\langle J_z\rangle$ and $Q = \langle O_2^0\rangle$ are the only nonzero average values and within the new tetragonal symmetry the Hamiltonian $\mathcal{H}$ must be written

$$\mathcal{H} = \mathcal{H}_{\text{CEF}} - g_J\mu_{\text{B}}(H + nM)J_z - B_1\epsilon_3 O_2^0 - K_1 Q O_2^0 + \left[\tfrac{1}{2}(C_{11}^0 - C_{12}^0)(\epsilon_3)^2 + \tfrac{1}{2}nM^2 + \tfrac{1}{2}K_1 Q^2\right] \; . \qquad (9)$$

The perturbation theory has to be carried out up to the second order for ϵ_3 and the fourth order for H in order to derive the analytical expression of the total free energy $F_{\text{tot}} = -k_B T \ln Z$ starting from the partition function Z (see Appendix)

$$F_{\text{tot}} = F_{\text{CEF}} - \tfrac{1}{2}\chi_0(H + nM)^2 - \tfrac{1}{2}\chi_2(B_1\epsilon_3 + K_1 Q)^2 - \chi_2^{(2)}(B_1\epsilon_3 + K_1 Q)(H + nM)^2 - \tfrac{1}{4}\chi_0^{(3)}(H + nM)^4 + \tfrac{1}{2}(C_{11}^0 - C_{12}^0)\epsilon_3^2 + \tfrac{1}{2}nM^2 + \tfrac{1}{2}K_1 Q^2 \; , \qquad (10)$$

where four CEF susceptibilities may be defined without any exchange interactions (their expressions are given in the Appendix): χ_0 is the usual magnetic susceptibility, χ_2 is the tetragonal strain susceptibility occurring in the elastic-constant calculations,[11] $\chi_2^{(2)}$ is a quadrupolar-field susceptibility, and $\chi_0^{(3)}$ a third-order magnetic susceptibility.[12]

The equilibrium values for M, ϵ_3, and Q are given by the conditions of minimization of the free energy

$$\frac{\partial F_{\text{tot}}}{\partial M} = \frac{\partial F_{\text{tot}}}{\partial \epsilon_3} = \frac{\partial F_{\text{tot}}}{\partial Q} = 0 \; . \qquad (11)$$

That provides a system of three linear equations, the solution of which leads to the following expressions:

$$M = \chi_M H + \chi_M^{(3)} H^3 \; , \qquad (12)$$

$$\epsilon_3 = \frac{B_1}{C_{11} - C_{12}^0} Q \; , \qquad (13)$$

$$Q = \chi_Q H^2 \; , \qquad (14)$$

with

$$\chi_M = \frac{\chi_0}{1 - n\chi_0} \; , \qquad (15)$$

$$\chi_M^{(3)} = \frac{\chi_0^{(3)}}{(1 - n\chi_0)^4} + 2G_1 \frac{(\chi_2^{(2)})^2}{(1 - n\chi_0)^4(1 - G_1\chi_2)} \; , \qquad (16)$$

$$\chi_Q = \frac{\chi_2^{(2)}}{(1 - n\chi_0)^2(1 - G_1\chi_2)} \; . \qquad (17)$$

In Eqs. (16) and (17) the parameter G_1 is defined[13]

$$G_1 = \frac{(B_1)^2}{C_{11}^0 - C_{12}^0} + K_1 \; . \qquad (18)$$

Note that we find again for the equilibrium value of ϵ_3 [Eq. (13)] the expression derived not within any perturbation theory.[7]

2. *Rhombohedral symmetry*

H is now applied along a threefold axis, e.g., [111]. This new symmetry (rhombohedral) implies that the nonzero average values are

$$\langle J_x\rangle = \langle J_y\rangle = \langle J_z\rangle \qquad (19)$$

and

$$\langle P_{xy}\rangle = \langle P_{yz}\rangle = \langle P_{zx}\rangle \qquad (20)$$

and that the following relation is verified:

$$\epsilon_{xy}=\epsilon_{yz}=\epsilon_{zx} \ . \tag{21}$$

In this case, it is more convenient to make a rotation of the coordinates axes so that [111] is the new z axis: in the new system only $M' = g_J\mu_B\langle J_z\rangle$ and $Q'=\langle O_2^0\rangle$ are nonzero, and the new Hamiltonian $\mathcal{H}'$ is written

$$\begin{aligned}\mathcal{H}' = {} & H_{\mathrm{CEF}} - g_J\mu_B(H+nM')J_z \\ & -\tfrac{1}{2}B_2\epsilon_{k1}O_2^0 - \tfrac{1}{12}K_2Q'O_2^0 \\ & + \left[6C_{44}^0(\epsilon_{k1})^2 + \tfrac{1}{2}nM'^2 + \tfrac{1}{24}K_2Q'^2\right] \ ,\end{aligned} \tag{22}$$

with $k1 = xy$, yz, or zx and the primes referring to the new system.

After carrying out the same perturbation theory as in Sec. II B 1, we obtain the total free energy F'_{tot}

$$\begin{aligned}F'_{\mathrm{tot}} = F'_{\mathrm{CEF}} & -\tfrac{1}{2}\chi'_0(H+nM')^2 \\ & -\tfrac{1}{2}\chi'_2(\tfrac{1}{2}B_2\epsilon_{k1}+\tfrac{1}{12}K_2Q')^2 \\ & -\chi_2^{(2)\prime}(\tfrac{1}{2}B_2\epsilon_{k1}+\tfrac{1}{12}K_2Q')(H+nM')^2 \\ & -\tfrac{1}{2}\chi_0^{(3)\prime}(H+nM')^4 \\ & +6C_{44}^0\epsilon_{k1}^2+\tfrac{1}{2}nM'^2+\tfrac{1}{24}K_2Q'^2 \ .\end{aligned} \tag{23}$$

Here $\chi'_0=\chi_0$ because of the isotropy of the (first-order) magnetic susceptibility in cubic symmetry, but the χ'_2, $\chi_2^{(2)\prime}$, and $\chi_0^{(3)\prime}$ values differ from the corresponding nonprimed susceptibilities, according to the new cubic CEF wave functions adapted to the rhombohedral perturbation Hamiltonian (their expressions, however, are the same as for tetragonal symmetry).

The new equilibrium conditions for M', ϵ_{k1}, and Q' are

$$\frac{\partial F'_{\mathrm{tot}}}{\partial M'}=\frac{\partial F'_{\mathrm{tot}}}{\partial \epsilon_{k1}}=\frac{\partial F'_{\mathrm{tot}}}{\partial Q'}=0 \ . \tag{24}$$

These lead to the expressions

$$M'=\chi'_M H+\chi_M^{(3)\prime}H^3 \ , \tag{25}$$

$$\epsilon_{k1}=\frac{B_2}{24C_{44}^0}Q' \ , \tag{26}$$

$$Q'=\chi'_Q H^2 \ , \tag{27}$$

with

$$\chi'_M=\frac{\chi_0}{1-n\chi_0}\equiv\chi_M \ , \tag{28}$$

$$\chi_M^{\prime(3)}=\frac{\chi_0^{(3)\prime}}{(1-n\chi_0)^4}+\frac{1}{6}G_2\frac{(\chi_2^{(2)\prime})^2}{(1-n\chi_0)^4(1-\frac{1}{12}G_2\chi'_2)} \ , \tag{29}$$

$$\chi'_Q=\frac{\chi_2^{(2)\prime}}{(1-n\chi_0)^2(1-\frac{1}{12}G_2\chi'_2)} \ , \tag{30}$$

the parameter G_2 being defined[13]

$$G_2=\frac{(B_2)^2}{4C_{44}^0}+K_2 \tag{31}$$

and the same remark can be made for the equilibrium value of ϵ_{k1} [Eq. (26)]. Returning to the fourfold axes system we finally obtain

$$\langle P_{k1}\rangle=\tfrac{1}{6}Q'=\tfrac{1}{6}\chi'_Q H^2 \ . \tag{32}$$

3. *Behavior of the magnetic quadrupolar susceptibilities*

a. Without CEF effects. The magnetic susceptibilities are known to reduce to [Fig. 1(a)]

$$\chi_0=\frac{C}{T} \ , \tag{33}$$

$$\chi_M=\frac{C}{T-\theta^*} \ , \tag{34}$$

where $C=g_J^2\mu_B^2[\frac{1}{3}J(J+1)]$ is the Curie constant and $\theta^*=nC$. In the same way, we obtain for the strain and quadrupolar susceptibilities

$$\chi_2=\chi'_2=\frac{1}{5T}J(J+1)(2J-1)(2J+3)=\frac{C_Q}{T} \ , \tag{35}$$

$$\chi_2^{(2)}=\chi_2^{\prime(2)}=\tfrac{1}{6}g_J^2\mu_B^2\frac{C_Q}{T^2} \ . \tag{36}$$

Let us define

$$\theta_Q^*=C_QG_1 \ , \tag{37}$$

$$\theta_Q^{*\prime}=C_Q(\tfrac{1}{12}G_2) \ , \tag{38}$$

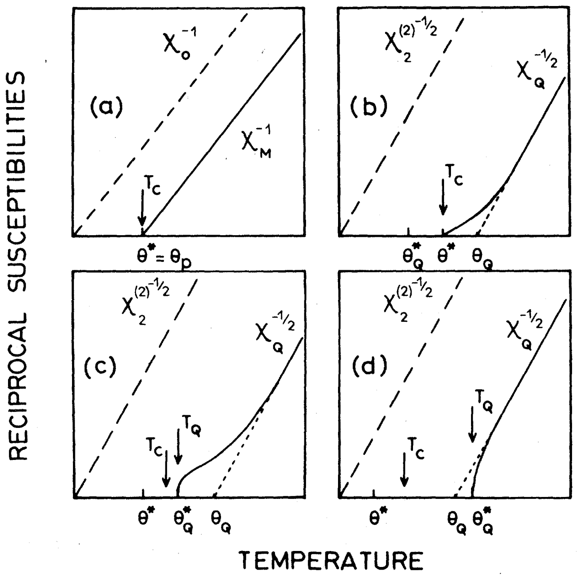

FIG. 1. Classical temperature dependences of the magnetic dipolar and quadrupolar reciprocal susceptibilities for various θ^* and θ_Q^* values.

which correspond to the structural transition temperature T_{cl}^* defined by Kataoka and Kanamori[14] in their elastic constants expression [Eq. (60), in Ref. 14]. The total quadrupolar susceptibility χ_Q [Eq. (17)] is then given by

$$\chi_Q = \tfrac{1}{6} g_J^2 \mu_B^2 \frac{C_Q T}{(T-\theta^*)^2 (T-\theta_Q^*)} \tag{39}$$

and the same expression for χ_Q' with θ_Q^* changed into $\theta_Q^{*\prime}$. As the reciprocal magnetic susceptibility [Fig. 1(a)], $\chi_Q^{-1/2}$ exhibits a linear T dependence at high temperature[2]; its extrapolation down to the T axis allows to define a "paraquadrupolar temperature" $\theta_Q = \theta^* + \frac{1}{2}\theta_Q^*$ [Figs. 1(b), 1(c), and 1(d)] which depends on both exchange parameters.

At low temperatures, $\chi_Q^{-1/2}$ deviates from the linearity, according to the relative values of θ^* and θ_Q^*. From Eqs. (15) and (17) [or Eq. (30)], two ordering temperatures T_C and T_Q associated with the two coefficients n and G_i may be defined by the vanishing of, respectively, χ_M^{-1} and $\chi_Q^{-1/2}$ (or $\chi_Q'^{-1/2}$), the transitions being here continuous. Two cases appear: (i) with $\theta^* \geqslant \theta_Q^*$, the dipolar ordering occurs at $T_C = \theta^*$ the quadrupoles being consequently ordered, this is the magnetostrictive process [Fig. 1(b)]. (ii) with $\theta_Q^* > \theta^*$, the quadrupoles alone order at $T_Q = \theta_Q^*$; below T_Q, the dipole ordering may occur at a T_C value depending on both θ^* and θ_Q^* [Figs. 1(c) and 1(d)].

b. In presence of CEF effects. The same high-temperature behavior occurs; however, additional deviations may be induced at low temperature by the character of the admixed CEF levels. In addition the simple identities $T_C = \theta^*$ or $T_Q = \theta_Q^*$ are not correct here: The relation between ordering temperatures and corresponding exchange parameters are more complex and depend on the exact CEF level scheme.

c. Parastriction formalism. Under an applied magnetic field, the total relative change of length λ can be expressed including the isotropic bulk anomaly ϵ_v as

$$\lambda = \frac{\delta l}{l} = \tfrac{1}{3}\epsilon_v + \frac{1}{\sqrt{6}}\epsilon_3(3\beta_3^2 - 1) + \frac{1}{\sqrt{2}}\epsilon_2(\beta_1^2 - \beta_2^2)$$
$$+ 2(\epsilon_{xy}\beta_1\beta_2 + \epsilon_{yz}\beta_2\beta_3 + \epsilon_{zx}\beta_3\beta_1) \;, \tag{40}$$

where the β_i's are the direction cosines of the measurement direction. In order to eliminate the ϵ_v effect, the magnetic field is successively applied parallel and perpendicular to the measurement direction. So for tetragonal deformation and according to Eqs. (13) and (14), measurements along a fourfold axis lead to:

$$\frac{H}{(|\lambda_\parallel - \lambda_\perp|)^{1/2}} = \left(\frac{2}{3}\right)^{1/4} \left(\frac{C_{11}^0 - C_{12}^0}{B_1}\right)^{1/2} |\chi_Q|^{-1/2} \; . \tag{41}$$

For rhombohedral deformation [Eqs. (26) and (27)], one obtains along a threefold axis

$$\frac{H}{(|\lambda_\parallel - \lambda_\perp|)^{1/2}} = 2\sqrt{2} \left(\frac{C_{44}^0}{B_2}\right)^{1/2} |\chi_Q'|^{-1/2} \; . \tag{42}$$

As a consequence of Sec. II B 3, the high-temperature slope of $H/(|\lambda_\parallel - \lambda_\perp|)^{1/2}$ gives the magnetoelastic coefficient B_i and the paraquadrupolar temperature θ_Q the G_i parameter, θ^* being known from the magnetic susceptibility. It is then possible to deduce K_i using Eq. (18) or (31). This parastriction method appears to be complementary with elastic constants which in the cubic paramagnetic range also gives G_i and K_i, then $|B_i|$.

III. PARASTRICTION RESULTS IN THE *R*Zn SERIES

Our *R*Zn parastriction data have been obtained with a capacitance dilatometer[15] under magnetic fields up to 3.6 kOe with a sensitivity of 1 Å and an accuracy of 1%; the size of our monocrystalline samples (about 5 mm) limits the relative change of length to 2×10^{-8}. At every temperature the quadratic field dependence of the measured strain has been checked. *R*Zn physical characteristics are reported in Table I.

TABLE I. Some physical characteristics in *R*Zn ferromagnets: Curie temperatures, cubic CEF parameters, and background elastic constants at room temperature.

*R*Zn	T_C (K)	θ^* (K)	$A_4\langle r^4\rangle$ (K/at.)	$A_6\langle r^6\rangle$ (K/at.)	$(C_{11}-C_{12})_0$ (10^5 K/at.)	$(C_{44})_0$ (10^5 K/at.)
TbZn	204		−41	−83	1.09	1.27
DyZn	139		−34	−33	1.2	1.44
HoZn	74	79	−14	−18	1.41	1.53
ErZn	20	26	−36	−18	1.74	1.65
TmZn	8.12	8.1	−38	−20	1.5	1.63
	$T_Q = 8.55$					

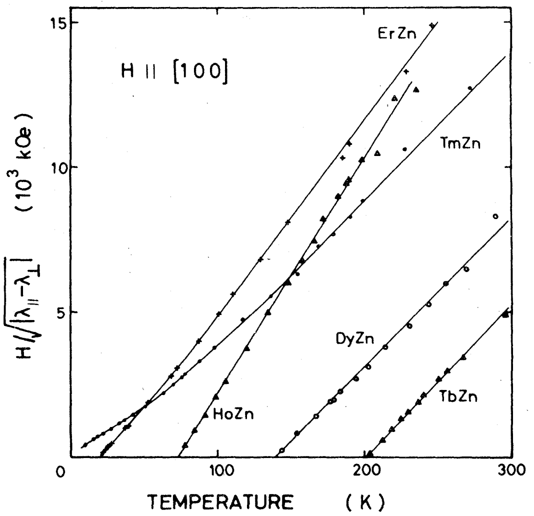

FIG. 2. Temperature variations of $H/(|\lambda_{\parallel}-\lambda_{\perp}|)^{1/2}$ for tetragonal strain in RZn. The full lines are calculated dependences.

A. Tetragonal strain

Figure 2 shows the temperature dependences of $H/(|\lambda_{\parallel}-\lambda_{\perp}|)^{1/2}$ obtained from TmZn to TbZn.

1. *TmZn*

This case is the best illustration of the wealth of parastriction. In this compound[3] the quadrupoles tetragonally order at higher temperature ($T_Q = 8.55$ K) than the magnetic dipoles ($T_C = 8.12$ K). In Eq. (2), W and x are known from neutron spectroscopy, $\theta^* = 8.1$ K from magnetic susceptibility. Then the quadrupolar susceptibility may allow the determination of G_1 from the experimental value of $\theta_Q = 30 \pm 2$ K [Fig. 3(a)]. Calculations show the sensitive dependence of θ_Q on G_1: for $\theta^* = 8.1$ K, the extrapolation down to the T axis of the high-temperature slope gives $\theta^* = 3$ and 30 K for, respectively, $G_1 = 0$ and 25 mK.

Note that $G_1 = 0$ would lead to the vanishing of $\chi_Q^{-1/2}$ at a second-order magnetic-ordering temperature $T_C = 3.6$ K, the curvature being negative. With $G_1 = 25$ mK, the structural transition temperature as well as its first-order character and the positive curvature of $\chi_Q^{-1/2}$ are described. The magnetoelastic coefficient is $B_1 = -27$ K, and the corresponding contribution to G_1 is $B_1^2/(C_{11}-C_{12})_0 = 4.8$ mK. Hence K_1 may be deduced to be about 20 mK; this indicates that the structural transition is driven by the quadrupolar exchange.

These coefficients are in fine agreement with other determinations: (i) the spontaneous strain ($c/a - 1 = -9 \times 10^{-3}$ at 4.2 K) has been fitted[3] with $B_1 = -25.5 \pm 1$ K. (ii) The ($C_{11}-C_{12}$) mode softening has led to $G_1 = 25 \pm 1$ mK, $K_1 = 20 \pm 1$ mK, and then $|B_1| = 28 \pm 3$ K.

2. *ErZn*

For this magnetostrictive compound, $H/(|\lambda_{\parallel}-\lambda_{\perp}|)^{1/2}$ cancels at $T_C = 20.5$ K. The high-temperature extrapolation leads to $\theta_Q = 31 \pm 2$ K. The best fit is obtained with $B_1 = -9.1 \pm 1$ K and $G_1 = 4 \pm 2$ mK [Fig. 3(b)]. Here too, they may be compared to their determination from ultrasonic data[16] ($G_1 = 2.9 \pm 0.3$ mK, $K_1 = 2.1 \pm 0.2$ mK, and

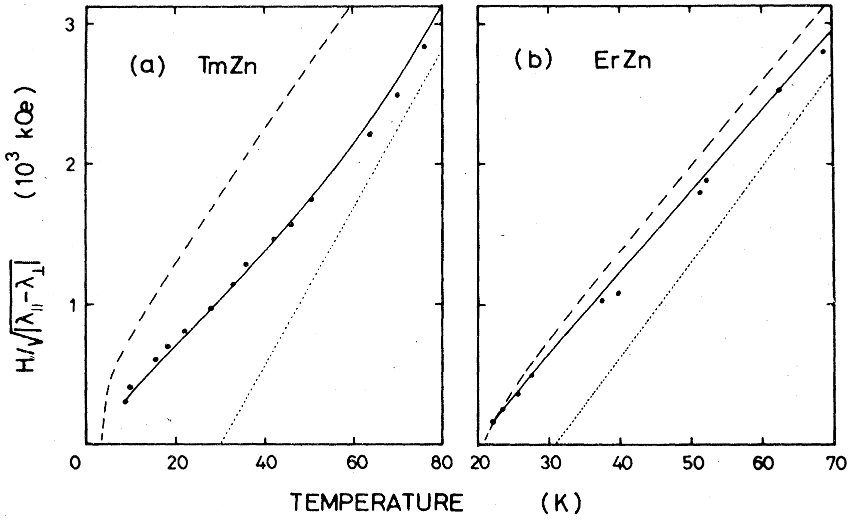

FIG. 3. Low-temperature variation of $H/(\lambda_{\parallel}-\lambda_{\perp})^{1/2}$ (tetragonal strain) – – –: $G_1 = 0$, and · · · · · · · ·: high-temperature extrapolation. (a) In TmZn ——$G_1 = 25$ mK and (b) in ErZn ——$G_1 = 4$ mK.

$|B_1|=11\pm3$ K). They allow a good description of the magnetization processes at low temperatures[13]

3. *HoZn*

The slope of $H/(|\lambda_{\parallel}-\lambda_{\perp}|)^{1/2}$ is the strongest one in the series, leading to the weakest magnetoelastic coefficient $B_1=3.6\pm1$ K [$B_1^2/(C_{11}-C_{12})\sim0.1$ mK]. The G_1 contribution can not be precisely obtained ($\theta_Q\sim\theta_p=75$ K) $G_1=0\pm5$ mK. The same conclusions may be derived from ultrasonic data when no softening is observed due to the weak magnetoelastic contribution. However the fit of the low-temperature magnetization processes[13] had given $G_1=-4\pm2$ mK.

4. *DyZn and TbZn*

Increasing θ^* has two main consequences: (i) the CEF effects, particularly spectacular at low temperatures, are hidden. (ii) As the investigated range is reduced, the high-temperature linear behavior, above deviation effects near T_C [Fig. 1(b)], may be unobserved, and the fit leads to only a relation between G_1 and K_1. In DyZn the possible (G_1, B_1) couples range from ($B_1=10.4$ K, $G_1=0$) to ($B_1=7.2$ K, $G_1=25$ mK). In TbZn, the corresponding limits are ($B_1=11$ K, $G_1=25$ mK). In TbZn, the corresponding limits are ($B_1=11$ K, $G_1=0$) and ($B_1=8.4$ K, $G_1=50$ mK).

B. Rhombohedral strain

The temperature variation of $H/(|\lambda_{\parallel}-\lambda_{\perp}|)^{1/2}$ in the five studied compounds is drawn in Fig. 4. The slopes are obviously steeper than for tetragonal strains (Fig. 2), indicating smaller rhombohedral changes of length. This necessitates a precise [111] orientation in order to avoid any tetragonal contribution to the observed strain. A misorientation would have introduced strong azimuthal variations of $\lambda_{\perp}$ which were never observed. The investigated temperature range is limited to the neighborhood of T_C (deviations range as in Fig. 1) and only a relation between B_2 and G_2 may be expected.

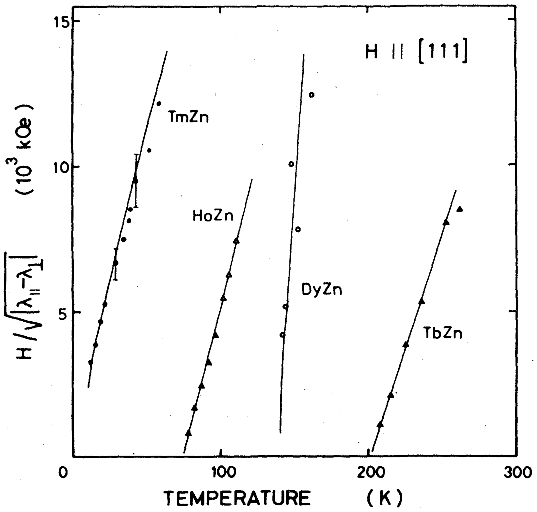

FIG. 4. Temperature variation of $H/(\lambda_{\parallel}-\lambda_{\perp})^{1/2}$ (rhombohedral strain) in *R*Zn.

TABLE II. Magnetoelastic and total second-order coefficients associated with rhombohedral symmetry.

*R*Zn	B_2 (K)	G_2 (K)
TbZn		
Parastriction	(+12, +20)	(0, −0.5)
Spontaneous strain[a]	11.6 ±0.8	
DyZn		
Parastriction	−0.5, −1.5	
HoZn		
Parastriction	(−4, −6.2)	(0, 0.1)
Spontaneous strain[a]	−6.4 ±0.4	0.0
ErZn		
Parastriction	not measurable	not measurable
TmZn		
Parastriction	(14, 34)	(−0.02, −0.5)

[a]Reference 7.

1. *TmZn*

The possible couples (B_2, G_2) range from ($B_2=14$ K, $G_2=-0.02$ K) to ($B_2=34$ K, $G_2=-0.5$ K). No agreement was possible with positive G_2 values; in addition, G_2 larger than 0.2 K would drive a rhombohedral structural transition above $T_Q=8.55$ K. Fitting the magnetization curves[3] along [110] and [111] led to $G_2=-0.07\pm0.05$ K; from magnetic excitations experiments G_2 was found[17] smaller than 0.04 K. The magnetoelastic contribution smaller than 1 mK is quite negligible in comparison with the quadrupolar exchange one, explaining the absence of any effect on the C_{44} mode.

2. *Other RZn*

In ErZn, no measurements of the weak ϵ_{xz} strain was possible. In HoZn, fitting the negative strain leads to couples ranging from ($B_2=-6.2$ K, $G_2=0$) to ($B_2=-4$ K, $G_2=0.1$ K). B_2 is then in good agreement with the determination from the strain in the ordered range (Table II). The possible G_2 range

TABLE III. Magnetoelastic, total second-order, and quadrupolar exchange coefficients associated with tetragonal symmetry.

*R*Zn	B_1 K	G_1 mK	K_1 mK
TbZn			
Parastriction	(11.1–8.4)	(0–50)	
Spontaneous strain[a]	15 ±1		
DyZn			
Parastriction	(10.4–7.2)	(0–25)	
Spontaneous strain[a]	16 ±2		
HoZn			
Parastriction	3.6 ±1	0 ±5	
Magnetization processes[b]		−4 ±2	
ErZn			
Parastriction	−9.0 ±1	4 ±2	−0.5
Elastic constants[c]	±11 ±3	2.9 ±0.3	2.1 ±0.2
Spontaneous strain[a]	−11.6 ±0.6		
TmZn			
Parastriction	−27 ±2	25 ±1	20 ±2
Elastic constants	±28 ±2	25 ±1	19 ±1
Spontaneous strain[d]	−25.5 ±1		
$T_Q = 8.55$ K		25 ±1	

[a] Reference 7.
[b] Reference 13.
[c] Reference 16.
[d] Reference 4.

includes the value deduced from magnetization processes[13] (+10 mK). In DyZn, B_2 is weakly negative (0, −1.5 K), no accuracy may be expected on G_2. In TbZn, B_2 ranges from +12 to +20 K for G_2 variations from 0 to −0.5 K. As in HoZn, we found again the B_2 value obtained with $G_2 = 0$ from the spontaneous strain, when the twofold axis is the easy magnetization direction.

IV. DISCUSSION

A. Magnetoelastic coefficients variation in the *R*Zn series

1. B_1 *variation*

The obtained magnetoelastic coefficients are given in Fig. 5. As it will be interesting to discuss them as CEF parameters, the B_1/α_J variation is also drawn. From Table III, some discrepancies appear with determinations from the spontaneous strain.[7] They originate from the overestimation of the two-ion magnetoelastic contribution in Ref. 7. This exchange coupling contributes to the tetragonal strain value by

$$\epsilon_3 = +\frac{D_1}{(C_{11}^0 - C_{12}^0)}\left(+2\langle J_z\rangle^2 - \langle J_x\rangle^2 - \langle J_y\rangle^2\right) . \quad (43)$$

The spontaneous strain observed in GdZn ($c/a - 1 = -4.5\times10^{-4}$ at 4.2 K; $B_1 = 0$) led to a $D_1 = -2.3$-K coefficient which was kept as a constant in the series. But having the same origin as θ^*, the two-ion magnetoelastic contribution must roughly vary as $(g_J - 1)^2 J(J+1)$ throughout the series for dominant $\vec{S}\,\vec{s}$ exchange interactions.

According to a de Gennes law, it contributes only about 10% to the total tetragonal strain in TbZn, where its effect is maximum (its relative contribution falls down to 3×10^{-2} and 10^{-3} in ErZn and TmZn, respectively). This two-ion magnetoelastic term is also present in the parastriction and then leads to a 10% underestimation of the positive value here deduced in TbZn: however, its separation from the one-ion coupling might be expected only at low temperature from CEF effects on the total parastriction temperature variation.

Neglecting this two-ion contribution in the formalism seems to be reasonable, keeping in mind that it may shift a little the one-ion magnetoelastic coefficient value (about 1 K/at. in TbZn). The temperature variation of the spontaneous strain as well as the parastriction is now described for each compound with the same B_1 value.

2. B_2 variation

As said above, the same B_2 values are obtained from the parastriction as from the spontaneous strain (Table II). The variation throughout the *R*Zn series is drawn in Fig. 5. If B_1/α_J remains negative, B_2/α_J changes in sign, which would be not expected from pure point-charge estimates. Since no reliable D_2 two-ion magnetoelastic coefficient had been detected in the ordered range of GdZn, this variation of B_2 cannot be explained by such a mechanism.

B. Conclusion

The application of parastriction to the *R*Zn compounds for the two main symmetry lowerings shows the possibilities of the method. Its quantum treatment is necessary in the case of cubic symmetry due to the wave-function mixing. It is particularly fruitful in presence of weak magnetic interactions, allowing a clear separation of the magnetoelastic coefficient and the quadrupolar exchange one. This may be successfully done for both the rhombohedral and tetragonal symmetries, since the moment can be aligned in any direction by an applied magnetic field.

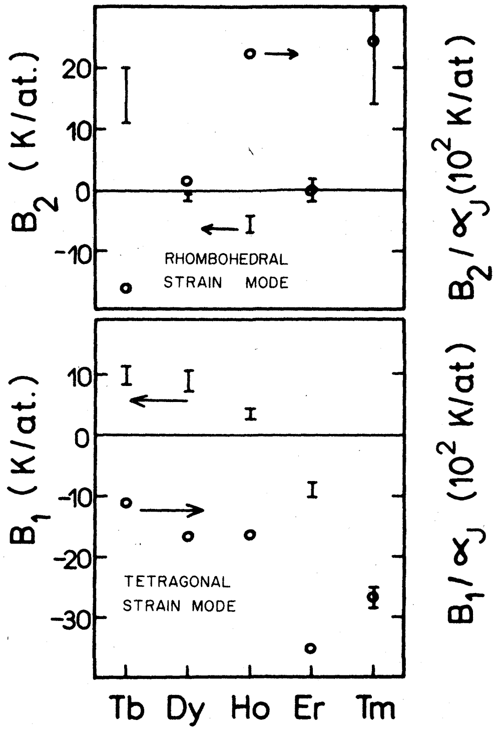

FIG. 5. Variation of the magnetoelastic coefficients in the *R*Zn series.

In comparison with sound-velocity measurements, a possible superiority is that parastriction may reveal a small magnetoelastic term simultaneously with a large quadrupolar exchange one, while no softening appears on the corresponding elastic constant. However, there is a great complementarity between the two methods, various measurements being necessary for determining reliably these high-rank parameters.

Performed in the disordered range, it is then developed under the same conditions as the neutron spectroscopy giving the cubic CEF parameters. In addition, the shortcomings of the exchange-interactions model are not felt here in the temperature variation of the dipolar and quadrupolar moments; thus parastriction allows also the study of magnetoelasticity in antiferromagnetic or more complex-magnetic-structure compounds.

The two sets of magnetoelastic coefficients obtained in *R*Zn lead to a result reminding us of the analysis of the fourth- and sixth-order CEF parameters[18]: they do not follow any scaling law throughout the series. This point is particularly emphasized by the rhombohedral magnetoelastic coefficient. They are strongly influenced by the anisotropic electronic structure, the influence of which will be tentatively discussed in a following paper.

APPENDIX

As a first stage we define the eigenvalues E_i and the eigenvectors $|ik\rangle$ corresponding to the Hamiltonian $\mathcal{H}_{\mathrm{CEF}}$ alone

$$\mathcal{H}_{\mathrm{CEF}}|ik\rangle = E_i|ik\rangle \ . \tag{A1}$$

In each subspace i the $|ik\rangle$ have to be adapted to the perturbation Hamiltonian. A perturbation theory up to the second order for ϵ_3 and the fourth order for H allows us to obtain the analytical expressions of the perturbed energies E_{ik}

$$E_{ik} = E_i + \sum_{n=1}^{4} E_{ik}^{(n)} + \cdots \ . \tag{A2}$$

Then the partition function Z

$$Z = \sum_{i,k} e^{-\beta E_{ik}} \tag{A3}$$

can be calculated (with $\beta = 1/k_B T$, k_B being the Boltzmann constant and T the temperature); one obtains

$$Z = Z_{\mathrm{CEF}}\{1 + \tfrac{1}{2}\beta\chi_0 H^2 + \tfrac{1}{2}\beta\chi_2(B_1\epsilon_3)^2 + \beta\chi_2^{(2)} B_1\epsilon_3 H^2 + \tfrac{1}{4}\beta[\chi_0^{(3)} + \tfrac{1}{2}\beta(\chi_0)^2]H^4 + \cdots\} \tag{A4}$$

that leads to the expression of the total free energy

$$F_{\rm tot}=k_BT\ln Z, \quad [\text{Eq.}(10)].$$

The expression of the four CEF susceptibilities χ_0, χ_2, $\chi_2^{(2)}$, and $\chi_0^{(3)}$ are given by

$$\chi_0=g_J^2\mu_{\rm B}^2\sum_{i,k}f_i\left(-2\sum_{j\neq i,l}\frac{|J_{ik,jl}|^2}{E_i-E_j}+\frac{1}{k_BT}|J_{ik,ik}|^2\right)\ , \tag{A5}$$

$$\chi_2=\sum_{i,k}f_i\left(-2\sum_{j\neq i,l}\frac{|Q_{ik,jl}|^2}{E_i-E_j}+\frac{1}{k_BT}|Q_{ik,ik}|^2\right)\ , \tag{A6}$$

$$\begin{aligned}\chi_2^{(2)}=g_J^2\mu_{\rm B}^2\sum_{i,k}f_i\Bigg[&\sum_{j\neq i,l}\sum_{j'\neq i,l'}\frac{J_{ik,jl}Q_{jl,j'l'}J_{j'l',ik}+2Q_{ik,jl}J_{jl,j'l'}J_{j'l',ik}}{(E_i-E_j)(E_i-E_{j'})}\\&-\sum_{j\neq i,l}\frac{|J_{ik,jl}|^2Q_{ik,ik}+2Q_{ik,jl}J_{jl,ik}J_{ik,ik}}{(E_i-E_j)}\left(\frac{1}{E_i-E_j}+\frac{1}{k_BT}\right)+\frac{1}{2(k_BT)^2}|J_{ik,ik}|^2\cdot Q_{ik,ik}\Bigg]\ ,\end{aligned} \tag{A7}$$

$$\begin{aligned}\chi_0^{(3)}=-\frac{1}{2k_BT}(\chi_0)^2+g_J^4\mu_{\rm B}^4\sum_{i,k}f_i\Bigg[&-4\sum_{\substack{j\neq i,l\\ j'\neq i,l'\\ j''\neq i,l''}}\frac{J_{ik,jl}J_{jl,j'l'}J_{j'l',j''l''}J_{j''l'',ik}}{(E_i-E_j)(E_i-E_{j'})(E_i-E_{j''})}\\&+2\sum_{\substack{j\neq i,l\\ j'\neq i,l'}}\frac{|J_{ik,jl}|^2|J_{ik,j'l'}|^2+2J_{ik,jl}J_{jl,j'l'}J_{j'l',ik}J_{ik,ik}}{(E_i-E_j)(E_i-E_{j'})}\left(\frac{2}{E_i-E_j}+\frac{1}{k_BT}\right)\\&-2\sum_{j\neq i,l}\frac{|J_{ik,ik}|^2|J_{ik,jl}|^2}{(E_i-E_j)}\left(\frac{2}{(E_i-E_j)^2}+\frac{2}{(E_i-E_j)k_BT}+\frac{1}{k_B^2T^2}\right)+\frac{1}{6k_B^3T^3}|J_{ik,ik}|^4\Bigg]\ ,\end{aligned} \tag{A8}$$

where

$$J_{ik,jl}=\langle ik|J_z|jl\rangle\ , \tag{A9}$$

$$Q_{ik,jl}=\langle ik|O_2^0|jl\rangle\ , \tag{A10}$$

are the matrix elements of J_z and O_2^0 between the cubic CEF levels. For each degenerate CEF level i,

$$f_i=\frac{1}{Z_{\rm CEF}}e^{-\beta E_i}=e^{-\beta E_i}/\sum_{i,k}e^{-\beta E_i} \tag{A11}$$

is the Boltzmann population factor.

---

[*] Laboratoire propre du C.N.R.S., associé á l'Université Scientifique et Médicale de Grenoble.

[1] G. T. Trammell, Phys. Rev. 131, 932 (1963).

[2] E. Callen and H. B. Callen, Phys. Rev. A 139, 455 (1965).

[3] P. M. Levy, P. Morin, and D. Schmitt, Phys. Rev. Lett. 42, 1417 (1979).

[4] P. Morin, J. Rouchy, and D. Schmitt, Phys. Rev. B 17, 3684 (1978).

[5] R. Aleonard and P. Morin, Phys. Rev. B 19, 3868 (1979).

[6] P. Morin, D. Schmitt, and E. du Tremolet de Lacheisserie, Phys. Lett. A 69, 217 (1978).

[7] P. Morin, J. Rouchy, and E. du Tremolet de Lacheisserie,

Phys. Rev. B 16, 3182 (1977).

[8] K. H. J. Stevens, Proc. Phys. Soc. London Sect. A 65, 209 (1952).

[9] R. Lea, M. J. M. Leask, and W. P. Wolf, J. Phys. Chem. Solids 23, 1381 (1962).

[10] B. Lüthi, in *Proceedings of the 1st Joint Magnetism and Magnetic Material-Intermag Conference, Pittsburg, 1976,* edited by J. J. Becker and G. H. Lander, AIP Conf. Proc. No. 34 (AIP, New York, 1976), p. 7.

[11] M. E. Mullen, B. Lüthi, P. S. Wang, E. Bucher, L. D. Longinotti, J. P. Maita, and H. R. Ott, Phys. Rev. B 10, 186 (1974).

[12] P. Morin and D. Schmitt, Phys. Lett. A 73, 67 (1979).

[13] P. Morin and D. Schmitt, J. Phys. F 8, 951 (1978).

[14] M. Kataoka and J. Kanamori, J. Phys. Soc. Jpn. 32, 113 (1972).

[15] E. du Tremolet de Lacheisserie, Rev. Phys. Appl. 10, 169 (1975).

[16] P. Morin, A. Waintal, and B. Lüthi, in *Proceedings of the 12th Rare Earth Research Conference, Vail, Colorado, 1976,* edited by U.S. Bureau of Mines (C. E. Lundin, Denver, 1976).

[17] P. Morin, D. Schmitt, C. Vettier, and J. Rossat-Mignod, J. Phys. F (to be published).

[18] D. Schmitt, J. Phys. F 9, 1745, 1759 (1979).